Deformation mechanism and fibre toughening of nylon 6,6

Ming-Liang Shiao and Shanti V. Nair*
Department of Mechanical Engineering, University of Massachusetts, Amherst, MA 01003, USA

and Paul D. Garrett and Robert E. Pollard
The Chemical Group of Monsanto Company, Springfield, MA 01151, USA
(Received 25 February 1993; revised 12 May 1993)

The effects of glass-fibre reinforcement on the fracture toughness, K_{IC}, of nylon 6,6 were examined and the deformation mechanisms of unreinforced nylon 6,6 were studied by varying the deformation rate, by dilatational measurements and by i.r. spectroscopy. In the unreinforced nylon 6,6 a flow stress plateau was observed in the stress–strain behaviour prior to the onset of necking. Of the 25–30% inelastic strains stored in this plateau a substantial portion appears to be related to a crystallographic plastic deformation due to the crystalline segments in nylon 6,6. In glass-fibre-reinforced nylon 6,6 a brittle to ductile transition was found to occur when the mean fibre-end spacing was less than a critical value. The observed brittle–ductile transition was found to originate from an observed enhanced matrix plasticity at fibre ends when the glass fibres are sufficiently closely spaced. Such enhanced localized plasticity at fibre ends was suggested to result from interactions of stress fields with nearby fibre ends when the fibre-end spacing is less than the critical value. It is further postulated that the enhanced localized fibre-end plasticity is made possible due to the ability of the matrix to exhibit a large degree of crystallographic plasticity. The toughening behaviour of fibre-reinforced nylon 6,6 was also compared qualitatively to that of rubber-toughened nylon 6,6 and a general principle for microstructural toughening in nylon 6,6 was addressed. Strategies for fibre toughening in fibre-reinforced nylon 6,6 were also discussed.

(Keywords: nylon 6,6; glass fibres; fracture toughness)

INTRODUCTION

Polyamide 6,6 or nylon 6,6 is a semicrystalline thermoplastic that has been widely used in engineering applications due to its many outstanding mechanical properties, possessing a good combination of high strength and ductility[1–3]. However, it is also known that when nylon 6,6 is loaded in the presence of a high-stress concentrator, such as a notch or crack tip, the failure resistance of the material can be greatly reduced, resulting in a relatively low fracture toughness[4,5]. In recent years, toughening of nylon 6,6 by rubber particles to prevent such brittle failure has been achieved successfully[6–11]. Wu[6] has shown that notched impact toughness of rubber toughened (RT) nylon 6,6 can be greatly enhanced when the interparticle distance of rubber particles is less than a critical value. The importance of the interparticle distance on the toughening behaviour of RT nylon 6,6 has also been confirmed by other investigators[9,10]. Wu[6,7] has suggested that when the distance between adjacent rubber particles is less than a critical value, the stress states in the interparticle ligaments around rubber particles interact considerably, giving rise to enhanced toughening. Such enhanced toughening does not appear to be limited to rubber particles as second phases. It has been reported[12–15] that the notched impact toughness and the plane-strain fracture toughness, K_{IC}, of nylon 6,6 can be significantly increased by adding sufficient amounts of glass fibres, e.g. above 30 wt%. Although the type of secondary phase added to nylon 6,6 differs drastically in the above-mentioned cases, it appears that in both cases the toughness of nylon 6,6 can be substantially increased.

In previous studies[15,16] we have shown that, owing to embrittlement effects at fibre ends, the fracture toughness, K_{IC}, of glass-fibre-reinforced nylon 6,6 can be significantly reduced when only small amounts of glass fibres are added. However, when the amount of added glass fibres is increased beyond a critical value, the fracture toughness, K_{IC}, of fibre-reinforced nylon 6,6 was found to be greatly increased as a result of an enhanced crack-tip deformation process zone[15], similar to the enhanced inelastic deformations known to be generated by second-phase rubber particles[6]. Such an increase in the crack-tip deformation zone was found to result from the increase of matrix plastic deformation at fibre ends in the crack front region[15], followed by overlap of fibre-end plastic zones[17].

In this paper, we investigate the analogy between fibre toughening and rubber toughening with a view to providing a broader understanding of microstructural toughening of nylon 6,6 by second-phase particle

* To whom correspondence should be addressed

0032-3861/94/020306-09

additions. In particular, the deformation mechanisms in nylon 6,6 are also investigated in detail and the critical dependence of the observed deformation mechanism on microstructural toughening is illustrated. General strategies for microstructural toughening of nylon 6,6 are also discussed.

EXPERIMENTAL

The material studied was fibre-reinforced poly(hexamethylene adipamide), or nylon 6,6 supplied by Monsanto Company. The materials examined were first extrusion compounded into pellets by dry blending glass fibres with nylon 6,6 pellets, and were then injection moulded into test samples. Glass fibres with two different fibre diameters, 9.5 and 13 μm, were examined. The glass fibres were surface treated by the glass supplier to provide compatibility with nylon 6,6. Seven loading levels of glass-fibre content, 0, 1, 5, 10, 20, 25, 30 and 40% by weight of the matrix, were investigated. In the case of nylon 6,6 reinforced by 9.5 μm diameter glass fibres, the specimens were made by a dilution process where the composites containing lower glass fibre contents were injection moulded by mixing pellets of pre-extruded 40 wt% nylon 6,6 composite with pure nylon 6,6. The composites obtained by the dilution process were found to have smaller fibre lengths as compared to the non-diluted composites, and also resulted in an approximately constant fibre-length distribution as the fibre content was varied[16]. In the case of nylon 6,6 composites with 13 μm glass fibres, both non-diluted and diluted composites were made, and the details of the materials were provided in our previous work[16]. The average fibre lengths in each of the nylon 6,6 composites are shown in *Table 1*. The average fibre lengths of the composites studied were determined by the linear analysis method on micrographs of extracted glass fibres, as has been discussed elsewhere[16]. The mean fibre-end spacing in fibre-reinforced nylon 6,6 is calculated by[16]:

$$d=\left(\frac{8f}{\pi d_f^3 S}\right)^{-1/3} \quad (1)$$

where d is the mean fibre-end spacing, f denotes the volume fraction of glass fibre, and d_f and S represent the diameter and aspect ratio of the glass fibre, respectively.

Tensile samples (ASTM D638 type I), 3.2 mm thick, and bend test specimens, 6.35 mm thick, for the fracture toughness measurements were injection moulded. To prevent the effect of moisture and light degradation, after injection moulding the specimens were stored in a hot-seamed high-density polyethylene bag and were then sealed in aluminized paper until testing. The moisture content of the specimens was found to be below 0.4 wt%.

The tensile properties of the materials studied were examined by the ASTM D638 procedure on a computerized Instron 3602 servohydraulic testing system. The plane-strain fracture toughness, K_{IC}, was determined by the three-point bend method on precracked bend bars, 6.35 mm thick[18]. The precracks were made by inserting a fresh razor blade into a machined slot, and the crack-to-width ratio, a/W, was limited to 0.45–0.55 for all tests. The thickness requirement for valid K_{IC} measurement was also checked by the formula specified in an ASTM procedure[18]. It was found that the thickness requirement was satisfied for all tests except for the case of unreinforced nylon 6,6, where the thickness used was slightly lower than required. Unless specified in the text, the testing rate used for the tensile and fracture toughness measurement was 5 mm min^{-1}.

To investigate the deformation mechanism, dilatational deformation of nylon 6,6 was studied by measuring the lateral and longitudinal strain during tensile loading[19]. The volumetric strain of the deformed nylon 6,6 was then calculated from[19]:

$$\frac{\Delta V}{V}=(1+\varepsilon_x)(1+\varepsilon_z)^2-1 \quad (2)$$

where ε_x denotes the strain in the loading direction and ε_z the strain in the lateral direction. The nature of the deformation in nylon 6,6 was also examined as a function of applied strain rate. The possibility of strain-induced phase transformation in nylon 6,6 upon loading was investigated by i.r. spectroscopy on strained thin films. Thin film samples of nylon 6,6 were compression moulded and dried in a vacuum oven at 90°C for 4 h before testing. The thin film samples were then loaded in a stretcher designed to fit into the chamber of an IBM IR/32 Fourier transformed i.r. spectrometer. The nominal strain of the sample was determined by the relative movement of the stretcher's grips. The moisture effects inside the i.r. chamber were controlled by flowing dry air for 15 min prior to testing. The sample was scanned both in the unstrained and strained condition and the results were analysed by the spectrometer interfaced with an IR 44 computer program.

RESULTS

Fracture toughness of fibre-reinforced nylon 6,6

The fracture toughness, K_{IC}, as a function of glass-fibre content for nylon 6,6 reinforced by 9.5 μm diameter glass fibres is shown in *Figure 1*. As can be seen, the addition of as little as 1 wt% glass fibres significantly reduced the fracture toughness of nylon 6,6. As the glass content was increased above about 10 wt%, however, the fracture toughness of the reinforced nylon 6,6 showed a strong increase from 2 up to 8 MPa m$^{1/2}$ in the nylon 6,6 containing 40 wt% glass. This result indicates a transition as the fibre content is increased from small to sufficiently large values. Similar trends in the fracture toughness of

Table 1 Average fibre length in glass-fibre-reinforced nylon 6,6

Glass fibre diameter (μm)	Moulding process	Average fibre lnegth (μm) at various glass fibre contents (wt%)						
		1	5	10	20	25	30	40
9.5	Diluted	230	249	216	238	204	243	266
13	Diluted	–	–	291	282	215	214	237
13	Non-diluted	–	–	380	364	–	263	232

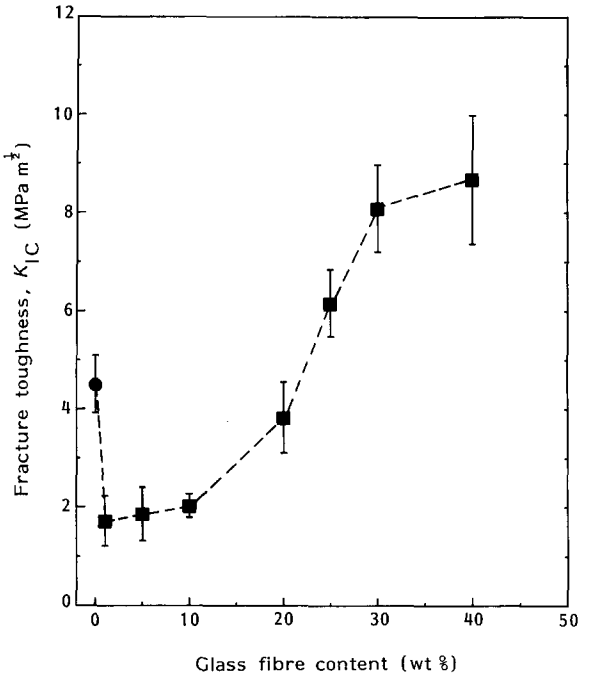

Figure 1 Fracture toughness, K_{IC}, *versus* glass-fibre content for diluted nylon 6,6 composite. ●, Unreinforced nylon 6,6; ■, nylon 6,6 reinforced by 9.5 μm diameter glass fibres

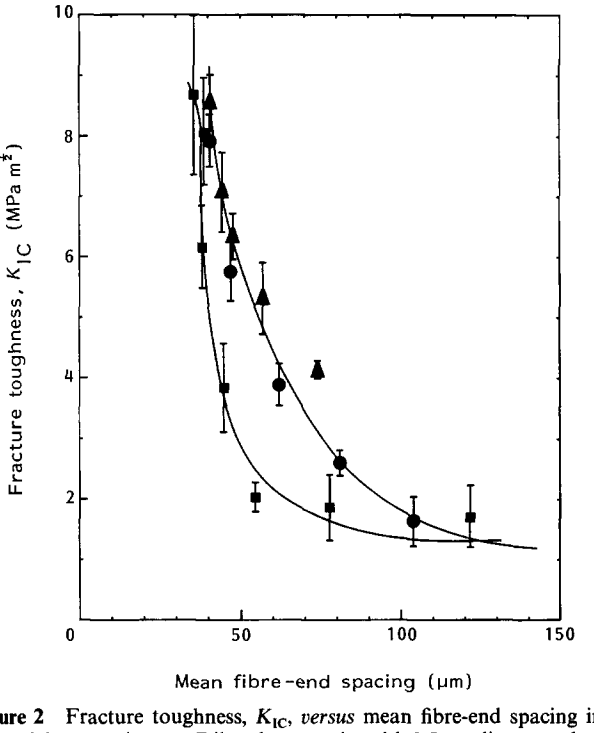

Figure 2 Fracture toughness, K_{IC}, *versus* mean fibre-end spacing in nylon 6,6 composites. ■, Diluted composite with 9.5 μm diameter glass fibres; ▲, diluted composite with 13 μm diameter glass fibres; ●, non-diluted composite with 13 μm diameter glass fibres

fibre-reinforced nylon 6,6 with 13 μm diameter glass fibres have also been observed and were reported in previous work[15]. However, it should be noted that when the smaller-diameter fibres were added, the fracture toughness was lower than that for the composite containing 13 μm diameter fibres in the regime of low fibre content, but was larger than that for 13 μm diameter fibres in the regime of high fibre content.

The fracture toughness, K_{IC}, as a function of mean fibre-end spacing, d, is shown in *Figure 2* for the nylon 6,6 composites reinforced by both 9.5 and 13 μm diameter glass fibres. As can be seen in both cases, the fracture toughness of the composites was relatively low when the mean fibre-end spacing, d, was large. However, the fracture toughness of both composites showed a sharp increase when the average fibre-end spacing was less than a critical value. This result suggests that there is a brittle to ductile transition, i.e. a brittle–ductile change of fracture mode in front of the crack tip, when the fibre-end spacing is decreased. Also, in the case of nylon 6,6 reinforced by 13 μm glass fibres, the fracture toughness for both the diluted and non-diluted composites shown in *Figure 2* was found to increase significantly at fibre-end spacings less than about 100 μm. In the case of nylon 6,6 reinforced by 9.5 μm glass fibres (diluted composite), the fracture toughness showed a substantial increase when the fibre-end spacing was less than about 70 μm. By normalizing the mean fibre-end spacing, d, with the fibre diameter, d_f, the fracture toughness values of the composites with different fibre diameters and dilution conditions were found to align into a single curve, see *Figure 3*. Note that in *Figure 3* the fracture toughness shows a brittle to ductile transition at d/d_f ratios less than about 6, i.e. the brittle to ductile transition occurs when the mean fibre-end spacing is less than about six times the fibre diameter. These results suggest that the mean fibre-end spacing relative to the fibre diameter may be a critical parameter in fibre toughening of fibre-reinforced nylon 6,6.

Deformation mechanisms in unreinforced nylon 6,6

The tensile stress–strain curves for unreinforced nylon 6,6 at three different test rates are shown in *Figure 4*. It can be seen that after yielding, two distinct constant-load plateau regions of deformation were observed in the stress–strain curves of nylon 6,6. Neck formation and propagation was found to coincide exactly

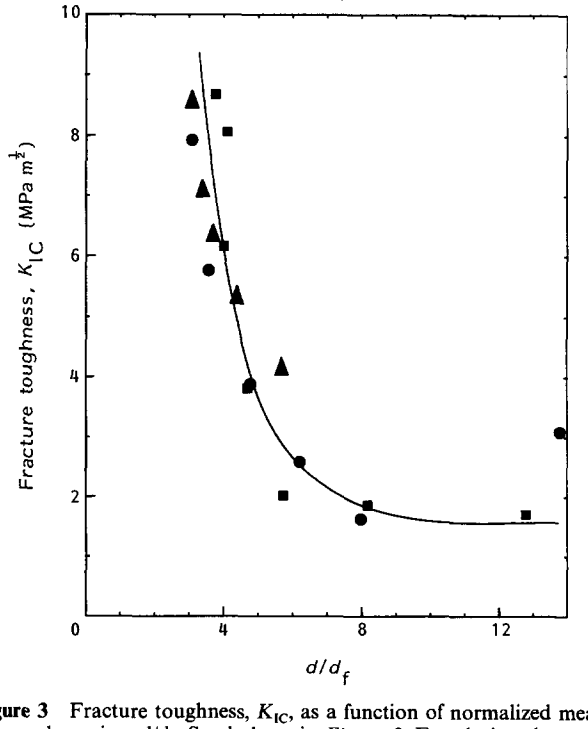

Figure 3 Fracture toughness, K_{IC}, as a function of normalized mean fibre-end spacing, d/d_f. Symbols as in *Figure 2*. For clarity, the error bars of data points are not shown

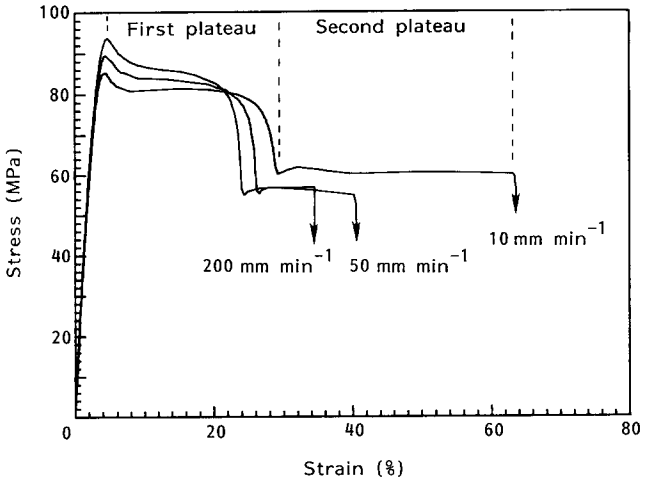

Figure 4 Stress–strain curves of nylon 6,6 at different test rates

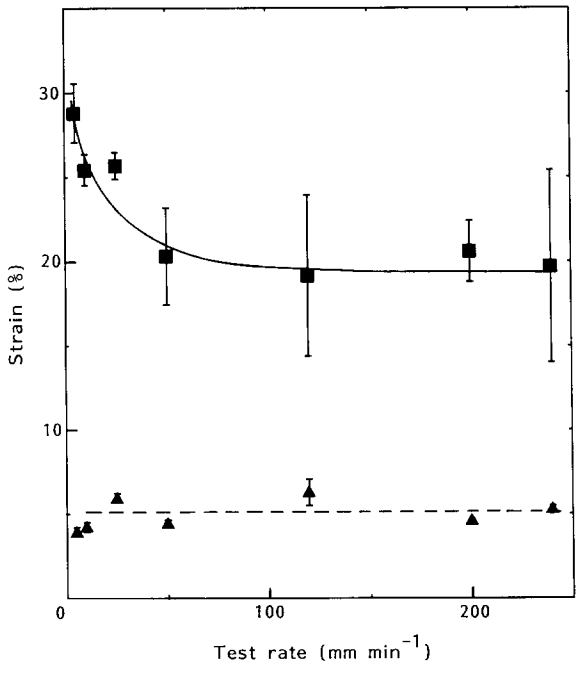

Figure 5 Effect of deformation rate on yield strain (▲) and the first-plateau strain (■) of unreinforced nylon 6,6

with the second plateau region, as has been noted previously by the authors[15]. Also note that in *Figure 4* the amount of deformation in the necking region (second plateau) was significantly reduced when the test rate was increased from 10 to 200 mm min^{-1}, whereas the amount of deformation in the first plateau was only slightly reduced by increasing the test rate. The effects of test rate on the amount of deformation accumulated in the first plateau and on the yield strain of nylon 6,6 are shown in *Figure 5*. Note that in *Figure 5* the amount of deformation accumulated in the first plateau showed an initial decrease when the test rate was increased, but then levelled off and remained at about 20% strain when the test rate was further increased above 50 mm min^{-1}. Also note that the increase of test rate had little effect on the yield strain of unreinforced nylon 6,6. On the other hand, the yield stress showed a significant increase when the test rate was increased, as can be seen in *Figure 6* where the yield stress, the first-plateau stress (the constant-load portion of the stress–strain curve) and the necking stress are plotted as a function of test rate. Note that in *Figure 6* the first-plateau stress was only slightly increased and tended to level off as the test rate was increased above 50 mm min^{-1}, whereas the necking stress showed an initial drop and approached a limiting value as the test rate increased.

The results of tensile dilatational measurements on the unreinforced nylon 6,6 are shown in *Figure 7*. As can be seen, the results indicate that little volumetric strain occurs during tensile deformation of unreinforced nylon 6,6 up to 30% tensile strain.

The i.r. spectra of unstrained and strained nylon 6,6 between wavenumbers 1400 and 500 cm^{-1} are shown in *Figure 8*. As can be seen in *Figure 8*, there is no indication of any new bands formed as nylon 6,6 is deformed into the first plateau region. Also, in the strained nylon 6,6 samples no shifting towards longer wavelengths was

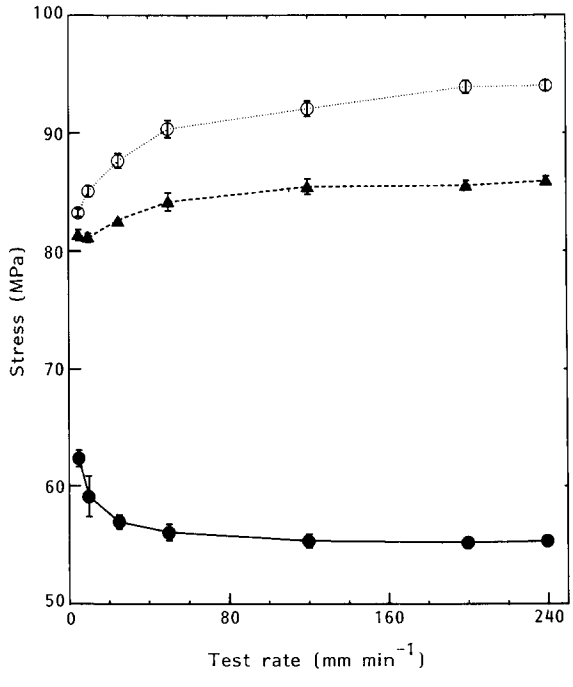

Figure 6 Effect of deformation rate on the yield stress (○), the stress for the first plateau (▲) and the stress for necking (●) of unreinforced nylon 6,6

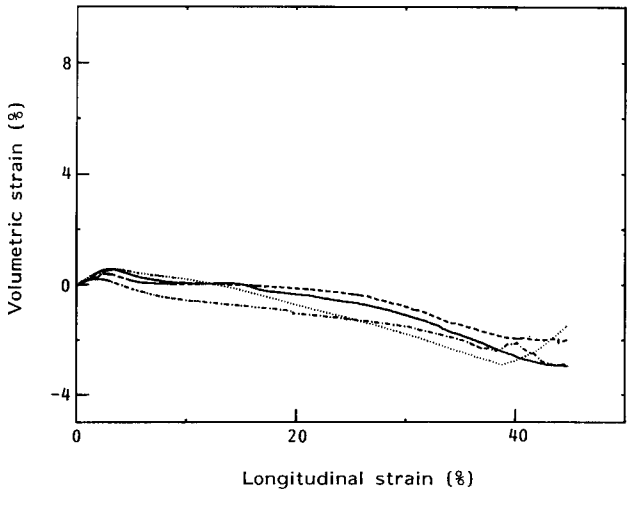

Figure 7 Tensile dilatational measurement of unreinforced nylon 6,6. ——, Test 1; - - -, test 2; — — —, test 3; —·—, test 4

recorded in the amide bands of planar α-forms near 690 and 580 cm^{-1}

DISCUSSION

The results shown in *Figures 2* and *3* clearly indicate that the mean distance between fibre ends or the mean fibre-end spacing, d, is a critical microstructural parameter in fibre toughening of nylon 6,6. This result can be considered as follows. With the addition of a small amount of glass fibres the fibre-to-fibre and fibre end-to-fibre end distances are large compared to the fibre diameter. Under these conditions, the stresses in the matrix would not be shielded by the presence of the fibres and the decrease in toughness is attributed to the observed debonding at fibre ends (see *Figure 9*) due to the presence of stress concentration at these sites[15,20,21]. The fracture toughness as a result of such an embrittlement effect at fibre ends has been derived to be related to microstructural factors according to[15]:

$$K_c = \sqrt{2\pi}\sigma^* \left(\frac{8f}{\pi d_f^3 S} \right)^{-1/6} \quad (3)$$

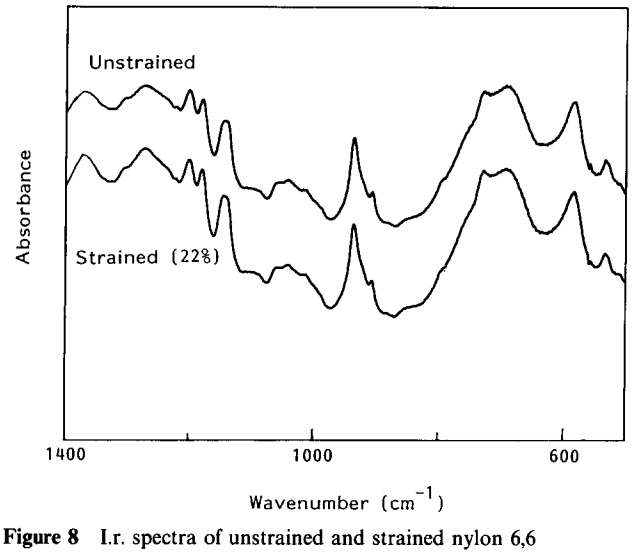

Figure 8 I.r. spectra of unstrained and strained nylon 6,6

where σ^* is the critical failure stress at fibre ends and is found to be approximately equal to matrix yield stress when equation (3) is fitted to the toughness data. The above equation indicates a sharp decrease of fracture toughness when small amounts of glass fibres are added[22], as has been observed in *Figure 1*. In this regime, the debonding at fibre–matrix interfaces may provide some toughening contributions. However, using an upper bound calculation, the magnitude of this toughness increase can be shown to be negligible, generally less than 5% of measured toughness values (see Appendix).

In contrast to the above case, when the amount of glass fibres is increased, the stress states at fibre ends can start to interact and failure was not observed to be dominated by fibre-end embrittlement effects. In fact, the results shown in *Figure 3* suggest that the brittle–ductile transition in fibre-reinforced nylon 6,6 takes place when the mean fibre-end spacing is less than about six times the fibre diameter. Photoelastic studies[23] on the stress states of glass fibres embedded in an epoxy resin indicated that the stress states around glass fibres cease to interact strongly with those of nearby fibre ends when the fibre-end distance is greater than six times the fibre diameter. Our previous *in situ* fracture observations have shown that plastic deformation at fibre ends was greatly enhanced when the fibre ends were more closely spaced, see *Figure 9*. Hence, the brittle–ductile transition in fibre-reinforced nylon 6,6 may appear to be due to the increasing matrix deformation at fibre ends from the interaction of overlapping stress fields with nearby glass-fibre ends. The increase of matrix plastic deformation in fibre-reinforced polymer can be assessed by calculating the expansion of the crack-tip fracture process zone, l_c, given by[15,24]:

$$l_c = \frac{C_1 C_2 K_{IC}^2}{\varepsilon_f^* \sigma_{yc} E_c} \quad (4)$$

where ε_f^* is the critical failure strain ahead of the crack tip, σ_{yc} and E_c are the tensile yield stress and modulus, respectively, and C_1, C_2 are constants[24]. It was found that l_c shows a significant increase from about one up to five or six times the mean fibre-end spacing

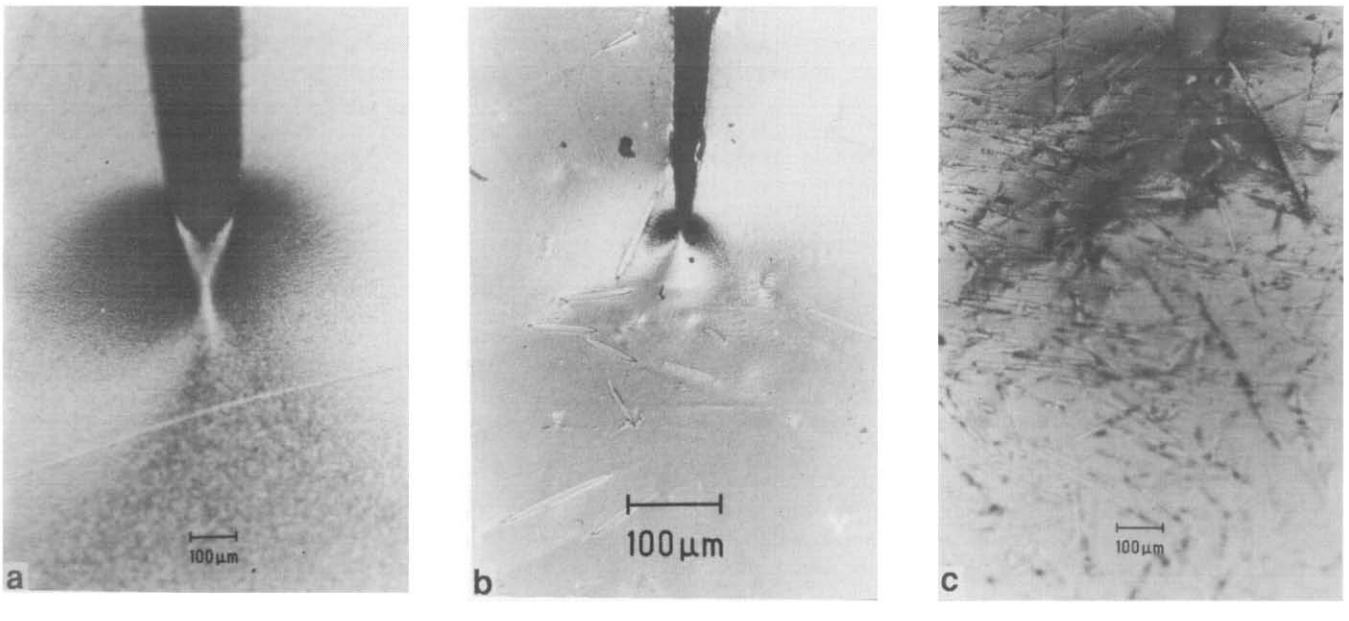

Figure 9 *In situ* fracture observations of crack-tip plasticity: (a) unreinforced nylon 6,6; (b) 5 wt% and (c) 30 wt% glass-fibre-reinforced nylon 6,6

as the composites pass through the brittle–ductile transition[15,22]. It is suggested that the larger fracture process zone results from the enhanced crack-tip blunting in the presence of the fibre-induced crack-tip plasticity. This result also confirms that the effect of glass fibres on the flow stress of the matrix, σ_{yc}, is alone not adequate to explain the magnitude of the toughness increase in *Figure 1*. Because of the enlarged fracture process zone in the high-fibre-volume case, there is the possibility that fibre-pull-out effects may contribute to toughness. However, an upper bound calculation for the fibre-pull contribution indicates that this contribution is small (see Appendix). Thus, the observed large increase in toughness is attributed directly to the crack-tip blunting and the increase in size of the fracture process zone.

The enhancement of the effective plastic zone size appears to occur by what is known as a percolation process. When the fibre volume fraction is small, the plasticity at fibre ends is separate and localized. However, when the fibre volume fraction increases, a stage is reached when the localized fibre-end plastic zones make contact. If the contacts are sufficient in number, the plasticity can be said to have 'percolated' through to a larger volume of the matrix. Percolation models[25] indicate that percolation is achieved rapidly over a narrow window, in this case of fibre volume fraction, giving rise to sharp changes in properties or threshold-type behaviour. This is consistent with the results indicated in *Figure 3*.

Correlation with RT nylon 6,6

As has been mentioned above, similar toughening behaviour to fibre-reinforced nylon 6,6 has also been encountered in notched Izod impact toughness results of RT nylon 6,6, where the surface-to-surface distance between rubber particles has been suggested as the only toughening criterion[6]. Although there can be differences between notched Izod impact and fracture mechanics tests, the fundamental deformation mechanisms are not expected to be altered. Other studies have also shown similarities in toughness trends between notched Izod and K_{IC} or J_{ic} results[26–28]. It is interesting to observe that in RT nylon 6,6 a transition from brittle to ductile failure in notched Izod impact toughness was observed as the rubber content increased, while keeping rubber particle size constant, see *Figure 10*. In the present case,

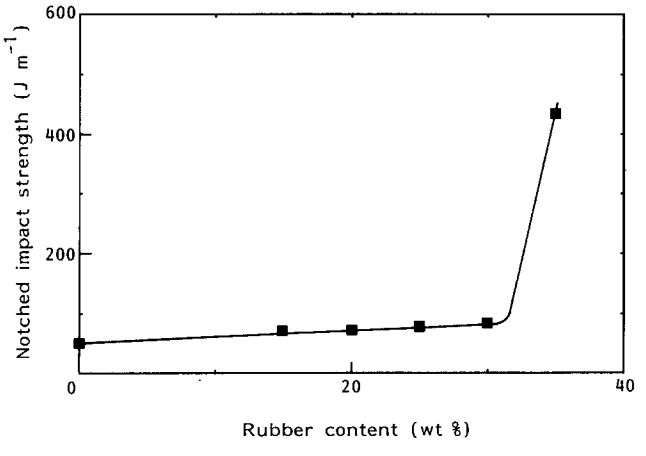

Figure 10 Effect of rubber content on impact strength of rubber toughened nylon 6,6 with constant rubber particle size. Data replotted from ref. 6

fracture toughness of nylon 6,6 reinforced by 9.5 μm glass fibres, shown in *Figure 1*, also showed a transition behaviour as the glass-fibre content increased, while keeping the fibre length the same, by preparing the specimens with the dilution process (see *Table 1*). In both cases, enhanced toughness was observed below a critical interparticle distance. As discussed above, in fibre-reinforced nylon 6,6, the toughness increase is related to the enhanced matrix plastic deformation at fibre ends. In the case of RT nylon 6,6, Wu[6,7] also noted that the increase in the impact energy of RT nylon 6,6 was mainly due to increased matrix yielding of nylon 6,6 around the rubber particles. Hence, the existence of a brittle–ductile transition and a critical interdistance between the secondary phase may be explained by the observation that in both cases the toughness is enhanced largely by localized plasticity associated with the second-phase particles. In RT nylon 6,6, a percolation model of stressed volume around rubber particles has been developed to explain the transition behaviour observed in Izod toughness[29]. The applicability of such a model to our results is being explored.

The magnitude of the critical surface-to-surface distance found in RT nylon 6,6 has been suggested as 0.3 μm[6]. In the fibre-reinforced nylon 6,6, however, the critical fibre-end spacing was on the order of 70 μm. This apparent difference can be resolved by considering the scaling effect in these two different secondary phases. In the case of RT nylon 6,6 the onset of the brittle–ductile transition occurs when the critical centre-to-centre particle distance, d_c, is less than[6]:

$$\frac{d_c}{d_r}=\left(\frac{\pi}{6\phi_r}\right)^{1/3} \tag{5}$$

where d_r denotes the particle diameter and ϕ_r is the volume fraction of rubber particles. In equation (5) it is seen that the ratio d_c/d_r is on the order of 1.7 to 1.4 for ϕ_r between 0.1 and 0.2, a comparable volume fraction range to the nylon 6,6 composites. It has also been suggested by Matsuo *et al.*[30] that the interaction of the stress fields around two rubber balls embedded in polystyrene occurs strongly when the ratio d_c/d_r is less than 1.45. In the case of fibre-reinforced nylon 6,6, the brittle–ductile transition starts to take place when the ratio d/d_f is less than 6, a factor about four times higher than that of RT nylon 6,6. This enhancement can be expected if one considers that the degree of stress concentration at fibre ends is considerably higher than that at a rubber particle[21]. Therefore, the stress states at fibre ends can interact strongly over a region of greater extent, which in turn requires a larger interparticle distance.

Since the above observation is derived from two extreme cases of reinforcement where the strength, stiffness, interfaces and shape of the reinforcements are entirely different, it is believed that a similar strategy for toughening of nylon 6,6 could be applied to other cases of reinforcement as well. Such observations can thus provide a general basis for microstructural toughening of nylon 6,6. It should be noted that the fracture toughness of unreinforced nylon 6,6 is relatively low in the presence of crack-tip high triaxial stress states, even though the ductility of nylon 6,6 is high. Accordingly, the critical issue in toughening nylon 6,6 by reinforcement appears to be the design of microstructures so that the enhanced matrix plastic deformation can be induced at crack tips

as a result of the stress states around the reinforcements in the crack-tip zone. The strategies for optimum design in fibre toughening of fibre-reinforced nylon 6,6 will be discussed below. The question still remains as to the nature of the inelastic deformation in nylon 6,6 and how it is related to the localized stress states. This is addressed in the next section.

Deformation mechanisms of nylon 6,6

As has been mentioned above, the origin of microstructural toughening in nylon 6,6 appears to be plastic deformation around the added secondary phase. In the case of fibre-reinforced nylon 6,6, even though the macroscopic strain to failure for nylon 6,6 composites is generally less than 7%[15], the microscopic matrix deformation near fibre ends can be very high[21,23] and is possibly well into the deformation region of the non-necking plateau portion of nylon 6,6 as shown in *Figure 4*. Hence an understanding of the deformation mechanism in the first plateau region of deformation can play an important role in the fibre toughening of nylon 6,6.

The results of dilatational measurements, shown in *Figure 7*, clearly indicate that the deformation in the first plateau region involves little volumetric strain. As a result, any dilatational deformation such as crazing in the amorphous phase or dilatational phase transformations is unlikely to be the major first-plateau deformation mechanism. In fact, the existence of the plateau region of deformation beyond yielding can also be observed during compression tests of nylon 6,6[31]. Thus, we conclude that the deformation in the first plateau region is mainly by shear deformation of nylon 6,6. The results shown in *Figures 2* and *3* suggest that the deformation of the first plateau region is unlikely to result totally from deformation in the amorphous phase of nylon 6,6. Since the deformation attributed to the amorphous content is expected to decrease significantly as the deformation rate increases, the existence of the first plateau region of deformation at test rates as high as 240 mm min^{-1} suggests that the first-plateau deformation is not primarily due to viscoelastic deformations in the amorphous phase. In fact, the results shown in *Figure 2* strongly suggest that the deformation in the first plateau is related to the deformation in the crystalline phase, since at least two-thirds of the first-plateau deformation is still remaining as the test rate is increased up to 240 mm min^{-1}. This conclusion is also consistent with our previous results on a hysteresis study done by unloading–reloading in the first plateau region, which showed that the hysteresis energy loss was associated with the crystalline component of nylon 6,6[15].

A possible mechanism of stress- or strain-induced phase transformation was suggested in an earlier work[15]; however, the i.r. spectroscopic study in this work did not provide any strong support of new phases formed during the deformation in the first plateau region. Although there appears to be a shifting and broadening of intensity between the band near wavenumbers 934 and 900 cm^{-1}, this apparent structural change is relatively small and can by no means account for the deformation accumulated in the first plateau (approximately 20–30% strain). Consequently, the only possible deformation mechanism for the first plateau appears to be a crystalline plastic deformation such as dislocation, slip or crystallographic twinning.

Evidence for twinning deformation in nylon 6,6 has been reported by Pope and Keller[32] using X-ray diffraction on compressed nylon 6,6. In their work, twinning deformation in nylon 6,6 was observed to operate at compressive strains of up to 30%, which correlates with the magnitude of the deformation observed in the first plateau region. However, it is still not clear that the magnitude of plastic deformation generated by as many as six twinning modes in nylon 6,6[32] would be sufficient to account for the first-plateau strain. It is also possible that successive twinning can be accomplished by reorientation of crystalline phase in the tensile direction during loading. Such a combined deformation mode may thus accumulate a large amount of plasticity by shearing of the crystalline phase. In a fibre-reinforced composite, due to the high deviatoric stress states generated at fibre ends[33] it is expected that this crystallographic twinning deformation would be enhanced preferentially at fibre ends. In particular, such deformation can be very significant when the deviatoric stress states at fibre ends interact strongly and can thus contribute substantially to the toughness of the composite.

Strategies of fibre toughening in nylon 6,6

The above results have shown that in fibre-reinforced nylon 6,6 the fracture toughness can be significantly enhanced when the mean fibre-end spacing is less than a critical value. On the other hand, the embrittlement effect at fibre ends can also reduce the fracture toughness by causing matrix cracking and early failure of the composite[15,20]. Hence, the degree of toughness enhancement in fibre-reinforced nylon 6,6 can be limited by the embrittlement effect at fibre ends. Due to the competing roles of the fibre ends, i.e. embrittlement effect on the one side and enhanced matrix plastic deformation through crystallographic plastic deformation on the other, it is necessary to reduce the embrittlement effect at fibre ends in order to further increase the toughness of a fibre-reinforced nylon 6,6. For example, controlling the fibre–matrix interface by introducing an interphase interlayer, which can enhance the deviatoric component of the stress concentrations at fibre ends, may provide a possibility for higher fibre toughening in nylon 6,6. Such interlayers may act as 'fuses' which bypass the embrittlement effects at fibre ends. The use of high strength fibre reinforcements, such as carbon fibres, may also significantly increase the fracture toughness of nylon 6,6 by increasing the fibre-end shear stresses to enhance the shear deformation of nylon 6,6.

The dimensions and orientation of glass fibres can also play an important role in the toughening of nylon 6,6. For instance, reducing the fibre diameter increases both the strength of glass fibres as well as the shear stresses at fibre ends[33], resulting in an increased fibre-end plasticity and higher fracture toughness[15]. However, the embrittlement effect at fibre ends can also be increased by the reduction of fibre diameter. This effect of fibre diameter is supported by our results, where the toughness is lowered in the small-volume-fraction regime as the fibre diameter decreased, but the toughness is increased in the regime of high fibre volume fraction by reducing fibre diameter. Also, for a given fibre content, the reduction in fibre length can increase the fibre-end density and thereby increase the possibility of fibre-end stress field interactions. As a result, the fracture toughness can be

increased, as has been observed previously[15]. The reduction of fibre length, however, can cause a lowering of strength and stiffness of the composite, thus reducing fibre strengthening efficiency. The effects of fibre orientation on the toughening behaviour of fibre-reinforced nylon 6,6 have not been carefully evaluated in this report and are thus an objective for future study.

Finally, the use of RT nylon 6,6 as a matrix for nylon 6,6 composites may increase the fracture toughness of the composite. However, it should be noted that the toughening capability of rubber particles in the composite can be substantially lowered by the shielding effects of glass fibres[26]. As a result, the composite may not have the desired toughness. The use of a multiphase hybrid composite with proper control of microstructures to enhance the stress states favoured for the first-plateau plastic deformation may provide a better way of toughening in reinforced nylon 6,6. It is believed that such microstructural toughening of nylon 6,6 can provide the possibility of desired toughness while maintaining the strength and stiffness of the material.

CONCLUSIONS

It was found that in glass-fibre-reinforced nylon 6,6, a brittle–ductile transition of fracture toughness, K_{IC}, occurred when the glass-fibre content was increased. The addition of small amounts of glass fibres reduced the fracture toughness of nylon 6,6; however, as the fibre content was increased above a critical level the fracture toughness was significantly increased.

The mean fibre-end spacing between glass fibres was found to be a critical parameter governing the brittle–ductile transition in fibre-reinforced nylon 6,6. The fracture toughness of fibre-reinforced nylon 6,6 was found to increase significantly when the mean fibre-end spacing is less than about six times the fibre diameter. In this respect, fibre toughening of nylon 6,6 has been found to be analogous to rubber toughening of nylon 6,6.

The observed increase in fracture toughness of fibre-reinforced nylon 6,6 was found to originate from an enhanced matrix plasticity at fibre ends in the crack tip region when the glass fibres were closely spaced.

In unreinforced nylon 6,6, the deformation mechanism responsible for a constant-load deformation after yielding, but prior to necking, was found to result from shear deformations in the crystalline phase. Such deformation modes constitute the enhanced matrix plasticity at fibre ends of nylon 6,6 composite and provide the general basis for microstructural toughening of nylon 6,6.

ACKNOWLEDGEMENTS

This work was supported by The Chemical Group of Monsanto Company, Plastics Division, Pensacola, Florida. Helpful discussions with Dr R. L. Kruse, Dr E. J. Kramer and Dr D. T. Grubb are also acknowledged.

REFERENCES

1 Chapman, R. D. and Chruma, J. L. in 'Engineering Thermoplastics' (Ed. J. M. Margolis), Marcel Dekker, New York, 1985, p. 83
2 Titow, W. V. and Lanham, B. J. 'Reinforced Thermoplastics', Applied Science, London, 1975, p. 38
3 Darden, E. T. in 'Nylon Plastics' (Ed. M. I. Kohan), John Wiley and Sons, New York, 1973, Ch. 20
4 Bonner, R. M., Kohan, M. I., Lacey, E. M., Richardson, P. N., Roder, T. M. and Sherwood Jr, L. T. in 'Nylon Plastics' (Ed. M. I. Kohan), John Wiley and Sons, New York, 1973, p. 345
5 McCrum, N. G., Buckley, C. P. and Bucknall, C. B. 'Principles of Polymer Engineering', Oxford University Press, Oxford, 1988, p. 329
6 Wu, S. *Polymer* 1985, **26**, 1855
7 Wu, S. *J. Polym. Sci. Polym. Phys.* 1983, **21**, 699
8 Bucknall, C. B. *Makromol. Chem. Macromol. Symp.* 1990, **38**, 1
9 Borggreve, R. J. M., Gaymans, R. J., Schuijer, J. and Ingea Housz, J. F. *Polymer* 1987, **28**, 1489
10 Borggreve, R. J. M., Gaymans, R. J. and Eichenwald, H. M. *Polymer* 1989, **30**, 78
11 Huang, D. D. *J. Mater. Sci.* 1987, **22**, 2503
12 Malzahn, J. C. and Friedrich, K. *J. Mater. Sci. Lett.* 1984, **3**, 861
13 Karger-Kocsis, J. and Friedrich, K. *Composite Sci. Technol.* 1988, **32**, 293
14 Titow, W. V. and Lanham, B. J. 'Reinforced Thermoplastics', Applied Science, London, 1975, p. 159
15 Shiao, M. L., Nair, S. V., Garrett, P. D. and Pollard, R. E. *J. Mater. Sci.* submitted
16 Shiao, M. L., Nair, S. V., Garrett, P. D. and Pollard, R. E. *J. Mater. Sci.* submitted
17 Sato, N., Kurauchi, T., Sato, S. and Kamigaito, O. *J. Mater. Sci.* 1991, **26**, 3891
18 Protocol on Plane-Strain Fracture Toughness and Strain Energy Release Rate of Plastic Materials, ASTM Subcommittee D20.10.27
19 Bucknall, C. B. 'Toughened Plastics', Applied Science, London, 1977, p. 195
20 Curtis, P. T., Bader, M. G. and Bailey, J. E. *J. Mater. Sci.* 1978, **13**, 377
21 Barker, R. M. and MacLaughlin, T. F. *J. Composite Mater.* 1971, **5**, 492
22 Nair, S. V., Shiao, M. L., Garrett, P. D. and Pollard, R. E. 'Mechanics and Mechanisms of Fracture in Glass Fiber Reinforced Semi-crystalline Thermoplastics', paper presented at ANTEC '93, Society of Plastic Engineers, New Orleans, 9–13 May, 1993, p. 2552
23 Schuster, D. M. and Scala E. in 'Fundamental Aspects of Fiber Reinforced Plastic Composites' (Eds R. T. Schwartz and H. S. Schwartz), John Wiley and Sons, New York, 1968, p. 45
24 Ritchie, R. O., Server, W. L. and Wulleart, R. A. *Metal. Trans.* 1979, **10A**, 1557
25 Stauffer, D. 'Introduction to Percolation Theory', Taylor and Francis, London, 1985
26 Nair, S. V., Shiao, M. L. and Garrett, P. D. *J. Mater. Sci.* 1992, **27**, 1085
27 Williams, J. G. 'Fracture Mechanics of Polymers', Ellis Horwood, Chichester, 1984, Ch. 8
28 Nair, S. V., Vestergaard, L., Shiao, M. L., Goettler, L. A. and Henry, W. D. 'Fracture Resistance of Unreinforced and Glass Fiber Reinforced PC/ABS Blends', paper presented at ANTEC '93, Society of Plastic Engineers, New Orleans, 9–13 May, 1993, p. 3279
29 Margolina, A. and Wu, S. *Polymer* 1988, **29**, 2170
30 Matsuo, M., Wang, T. T. and Kwei, T. K. *J. Polym. Sci. A-2* 1972, **10**, 1085
31 Bonner, R. M., Kohan, M. I., Lacey, E. M., Richardson, P. N., Roder, T. M. and Sherwood Jr, L. T. in 'Nylon Plastics' (Ed. M. I. Kohan), John Wiley and Sons, New York, 1973, p. 342
32 Pope, D. P. and Keller, A. *J. Mater. Sci.* 1975, **10**, 747
33 Piggott, M. R. 'Load-Bearing Fibre Composites', Pergamon, Oxford, 1980, Ch. 4
34 Wells, J. K. and Beaumont, P. W. R. *J. Mater. Sci.* 1985, **20**, 2735
35 Kim, J. K. and Mai, Y. W. *Composite Sci. Technol.* 1991, **41**, 333
36 Lauke, B., Schultrich, B. and Pompe, W. *Polym.-Plast. Technol. Eng.* 1990, **29**, 607
37 Kelly, A. and Tyson, W. R. *J. Mech. Phys. Solids* 1965, **13**, 329
38 Folkes, M. J. and Wong, W. K. *Polymer* 1987, **28**, 1309

APPENDIX

Toughness increase due to interfacial debonding and fibre pull-out

The fracture energy of a composite can be increased by the fibre–matrix interfacial debonding[34,35]. The energy absorption per unit area due to fully debonded

Table 2 Comparison of toughness data with calculated debonding and pull-out energy

Fibre type	Glass fibre content (wt%)	K_{IC} (MPa m$^{1/2}$)	G_c (kJ m^{-2})	G_i (kJ m^{-2})	G_p (kJ m^{-2})
9.5 μm glass fibres, diluted	10	2.04	1.97	0.21	0.96
	20	3.84	4.46	0.47	2.31
	25	6.17	8.11	0.56	2.36
	30	8.08	13.05	0.75	3.82
	40	8.68	13.28	1.17	6.50
13 μm glass fibres, diluted	10	4.14	6.97	0.21	0.94
	20	5.31	8.55	0.44	1.88
	25	6.34	10.44	0.43	1.41
	30	7.07	12.20	0.53	1.73
	40	8.56	13.85	0.84	3.03
13 μm glass fibres, non-diluted	10	2.61	2.66	0.28	1.61
	20	3.89	4.22	0.57	3.13
	30	5.78	7.07	0.65	2.61
	40	7.93	8.56	0.82	2.90

fibres, G_i, is given by[34]:

$$G_i = 4S\Gamma_i f \tag{6}$$

where Γ_i is the interfacial fracture energy and is on the order of 40–50 J m^{-2} (refs 34, 36). The fracture energy due to interfacial debonding, G_i, can thus be calculated by equation (6) and is listed in *Table 2*. Also listed in *Table 2* are the experimental data of energy release rate, G_c, calculated from the K_{IC} data of nylon 6,6 composites using:

$$G_c = \frac{K_{IC}^2}{E_c}(1-\nu^2) \tag{7}$$

where E_c is the tensile modulus of the composites and the Poisson's ratio, ν, is about 0.3. As can be seen in *Table 2*, the increase of fracture toughness in nylon 6,6 composites due to interfacial debonding is relatively small.

It is also known that the fracture energy of the composites can be increased by pull-out effects of glass fibres. The fracture energy due to complete pull-out of fibres, G_p, is approximately equal to [37]:

$$G_p = \frac{f d_f \tau_i S^2}{6} \tag{8}$$

where τ_i is the interfacial shear strength. In E-glass fibres embedded in polypropylene the value of τ_i has been measured[38] to be on the order of 20–30 MPa and has also been suggested to be about 0.3 of the matrix yield stress[36]. The G_p value as a function of fibre content is thus calculated using $\tau_i = 25$ MPa and is also listed in *Table 2*. As can be seen, the upper bound estimation of fracture energy due to pull-out is not adequate to explain the observed toughness increase as the fibre content increases. Also, the pull-out energy obtained in equation (8) is derived for uniaxially aligned fibres and does not account for the randomness of fibre orientation in the short-glass-fibre composites, which actually tends to further reduce pull-out contributions. Hence, the toughness contribution to K_{IC} by interfacial debonding and fibre pull-out may not be as significant.